Impact of Gamma Irradiation on Structural and Dielectric Properties of CuI-PVA / PEDOT: PSS Polymer Nanocomposite

M. E. Gouda*, T. Y. Elrasasi,

Physics Department, Faculty of Science, Benha University, Benha, Egypt.

Abstract: *Polymer nanocomposite of CuI-PVA/PEDOT: PSS has been prepared as solid layers by solution casting technique. The obtained polymer composite layers were irradiated with γ – rays at various doses to investigate the radiation effect on ac conductivity and dielectric permittivity in the frequency range of 0.1-100 KHz at different temperatures. The change in chemical interaction, morphology, and thermal properties was analyzed with the help of Fourier transform infrared spectroscope (FT-IR), Scanning electron microscopy (SEM) and thermogravimetric analysis (TGA) techniques, respectively, before and after irradiation. The chemical change was confirmed from the FT-IR result which showed a new peak appeared at720 cm^{-1} by irradiation which is characterized by, methylene Rocking (CH_2). The SEM images give that surface roughness increase with decreasing dose. The XRD pattern of all irradiated samples reveals a new sharp peak. It can be attributed to formation of a new phase (salesite) inside the polymer composites by gamma irradiation. Further, it is seen that maximum ac conductivity has been achieved for irradiated CuI-PVA/PEDOT: PSS polymer nanocomposite by 2 M rad, which can be attributed to, free radical formation. The ac conductivity, σ_{ac}, were found to obey the universal power law. The frequency exponent (s) parameter shows temperature dependent behavior which predicts the correlated barrier hopping (CBH) model is the most suitable model to characterize the electrical conduction mechanism for the present polymeric system.*

Keywords*: Polymer nanocomposite, Gamma irradiation, Dielectric properties.*

I. Introduction

Organic/inorganic polymer nanocomposites are extremely promising for the modern applications in smart microelectronics devices, light emitting diodes, photodiodes, and photovoltaic cells [1]. These advanced nanocomposites have many advantages such as low cost production and the possibility of device fabrication on large scale and flexible substrates. Solar cells composed of hybrid conjugated polymers and semiconductor nanocrystals can combine attractive characteristics of bulk inorganic materials and with the solution processability and low temperature chemical synthesis of polymers [2]. Furthermore, polymers, on doping with inorganic nanoparticles, show novel and distinctive properties obtained from unique combination of the inherent characteristics of polymers and properties of nanoparticles [3].

Cuprous Iodide (CuI) has attracted a great attention, as it is a versatile candidate in band gap materials (CuI, CuSCN, and $CuAlO_2$) were identified in the preparation of optical properties of thin film. CuI belongs to the I–VII semiconductors with Zinc blend structure. Conducting and optically transparent films aroused much interest in the capability of application in electronic devices such as liquid crystal displays, photovoltaic devices, photothermal collectors and etc…. The most interesting nature of this compound is that an inorganic semiconductor and its coordination chemistry let it readily couple with many inorganic and organic ligands as well [4-7].

A poly vinyl alcohol polymer (PVA) is a potential material having high dielectric strength, good charge storage capacity and dopant-dependent electrical and optical properties. The OH groups in the PVA structure could be the source of the hydrogen bonding and hence assist the formation of polymer composite by growing inorganic nanoparticles inside polymer matrix [8-10].

Poly(3,4-ethylenedioxythiophene) doped with poly(4-styrene-sulfonate) (PEDOT:PSS) has been used as a conducting shell for CuI/PVA core [11,12] which showed changes in physical properties of CuI-PVA/PEDOT:PSS composite. This study illustrated a change from ionic to electronic conductivity due to the reduction of CuI – PVA interface which enhance hole transportation through the polymer composite matrix. However, this result encouraged us to use gamma irradiation of the polymer composite under investigation to produce new electronic defects which may enhance conduction in the polymer composite.

Our previous work on preparation and characterization of CuI/PVA polymer composites illustrated their promising application as electron donor in photovoltaic solar cells [8]. The CuI in PVA plays an important role of the physical properties of CuI/PVA composite matrix; however, we have used (Tetramethlethylenediamine) TMED ligand as a dispersant agent.

Gamma radiation process for modification of commercial polymers is a widely applied technique to promote new physical, chemical and mechanical properties [13]. The irradiation of polymeric materials with ionizing radiation (gamma rays, X-rays, accelerated electrons and ion beams) leads to the formation of very reactive intermediates, free radicals, ions and excited states [14-17]. These intermediates can follow several reaction paths that result in molecular chains crosslinking, and/or destruction and degradation of the macromolecules with the simultaneous formation of molecules of smaller chain lengths and change in the number and nature of double bonds [18]. The degree of these transformations depends on the structure of the polymer and the conditions of treatment before, during and after irradiation. Those factors may be controlled in order to facilitate the modification of polymers by radiation processing .The radiation not only alters the chemical structure of the polymer, but it can also enhance the presence of trapped charges or creates defects in the polymer matrix changing the dielectric, electrical and thermal properties of irradiated polymer [19, 20]. Therefore, the field of ionizing radiations is an interesting field of research as an approach for the preparation of materials with enhanced properties.

The present study is aiming to study the effect of gamma irradiation on the structure and the electrical properties of CuI-PVA/PEDOT: PSS polymer nanocomposite.

II.   Experimental

PVA used in the present study was purchased from by Sigma-Aldrich and the other chemicals were provided by QualiKems Chemical Company, India. A PVA solution was prepared by adding deionized distilled water to 5 gm of PVA ($-C_2H_4O)_n$ (where n =30,000-70,000, average molecular weight) and then stirred by a magnetic stirrer at room temperature, 30°C, for 2 hrs. Then a solution of CuI in acetonitrile (10%) was added into a solution of PVA in dimethl sulfoxide (DMSO) under constant stirring for 2 hrs drop wise. Then 0.5 ml of TMED as a dispersant agent was added to obtain nano polymer composite followed by stirring for another 2 hrs at 70 ^{0}C to evaporate the acetonitryle solvent. Then composite colloidal was left to cool to room temperature which blended with appropriate amount of 4 ml aqueous solution of PEDOT: PSS (solid concentration, 1.2%). The as prepared polymer composite was directely casted in a Petri - glass dishes and left for 24 hrs at 50 ^{o}C to dry.

One of the prepared films was lift without irradiation, and the other four films were irradiated. Irradiation was performed using a Co-60 γ-source at a dose rate about 10 k rad/min. Irradiation cell installed at the National Center for Radiation Research and Technology (NCRRT) at the Egyptian Atomic Energy Authority (AEA). The irradiation process was performed in air, at room temperature, where a cooling system was used in the irradiation chamber to avoid heating of the samples during irradiation. The gamma irradiation was conducted at 0.5, 1, 2 and 4 M rad, respectively.

In order to investigate the structure of the polymer composite layers, X-ray diffraction studies were carried out using SHIMADZU diffractometer type XRD 6000, wave length λ=1.5418A°.

For IR measurement, a Fourier transform infrared (FT-IR) Perkin Elmer spectrometer model 1650 with scanning rate of 4 cm^{-1}s^{-1} was used in the energy range 400-4000 cm^{-1}.

In addition, the surface morphology of these nanocomposites was also examined using scanning electron microscope, SEM (JOEL-JSM Model 5600). Thermal analysis was carried out using a computerized TGA, TA-50 Schimadzu Corporation, Kyoto, Japan at heating rate 10 K/min. TGA is carried out at temperature range from 0 ^{0}C to 600 ^{0}C under nitrogen gas.

The CuI-PVA/PEDOT: PSS polymer nanocomposite thick layers of thickness of about 0.4 mm were used to measure the ac conductivity. The silver paste was used as conducting electrodes. Electrical measurements were carried out using PM 6304 programmable automatic RCL Philips meter in the frequency range 0.1 to 100 kHz.

III.   Results and Discussion

3.1 X-ray Diffraction

The XRD patterns of the as-prepared CuI-PVA/PEDOT: PSS polymer nanocomposite with different doses of gamma radiation is shown in Fig. 1. One notices that a broad peak appeared around 2θ = 19.36° which is the characteristic peak for PVA. Other peaks at 2θ = 13.8, 27.56°, 32° and 42.24° appeared which refer to the growth of CuI nano crystallite inside the PVA polymer matrix. The obtained results are in agreement with Hodge et al [21]. The diffraction peaks for CuI as mentioned above correspond to the (012), (110) and (202) planes of CuI nanocrystals which could be indexed to hexagonal structure (the lattice constants are: a= 4.0826 Å, c = 20.0770 Å) which were consistent with the literature data of JCPDS 83-1145. As the CuI-PVA/PEDOT:PSS polymer nanocomposite irradiated with different doses of gamma radiation, new sharp peak at 20.68° was appeared, indicating the growth of new phase of CuI crystallite nanoparticles in the polymer matrix. It can be attributed to formation of salesite phase ($CuHIO_4$) inside the polymer composites by irradiation (JCPDS 83-1145). The intensity of this new peak is relatively high at doses 1 and 4 M rad, while the minimum

intensity was at 2 M rad. The average particle size of CuI nanocrystals has been calculated according to the first sphere approximation of Debye–Scherrer formula [22].

$$D = \frac{0.9\lambda}{B\cos\theta} \qquad (1)$$

where, D is the average diameter of the particle, λ is the wavelength of the used X-ray radiation and B is the full width at half maximum intensity of the peak. The obtained values of particle size of CuI embedded in polymer composite for different gamma radiation doses lie in the range 28 and 58.5 nm with an average value = 43.4 nm. The variation of the particle size of CuI in general is attributed to the nano particles aggregations and the different interactions between CuI nano particles and the polymer chains due to the gamma radiation. From Table 1 one can see that dose 2 M rad has minimum particle size comparable to the other doses.
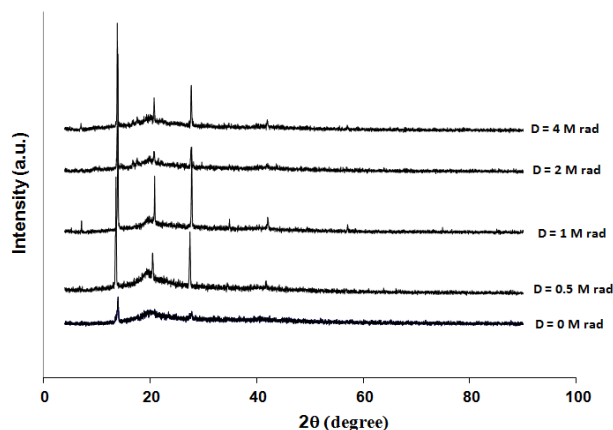
Fig. 1 XRD pattern for CuI-PVA/PEDOT: PSS polymer nanocomposite irradiated with different gamma doses 0, 1, 2, and 4 M rad.

Table 1 Extracted particle size D and the electrical activation energy E_a for CuI-PVA/PEDOT: PSS gamma irradiated polymer nanocomposite with different doses.

Dose , M rad	0	0.5	1	2	4
D , nm	28	45.5	58.5	37	48
E_a, eV at 20 KHz	0.420	0.414	0.476	0.489	0.358

3.2 FT-IR Analysis

Fig. 2 illustrates the FT-IR spectra of un-irradiated and irradiated CuI-PVA/PEDOT: PSS polymer nanocomposite films. The chemical changes due to gamma irradiation can be studied from the changing of the peaks intensity and the frequency shifts compared with the un-irradiated film. These changes for different peaks are listed in Table 2. It can be observed C–H broad alkyl stretching band (n = 2850-3000 cm^{-1}) and typical strong hydroxyl bands for free alcohol (non-bonded –OH stretching band at n=3600-3650 cm^{-1}), and hydrogen bonded band (n=3200-3570 cm^{-1}).
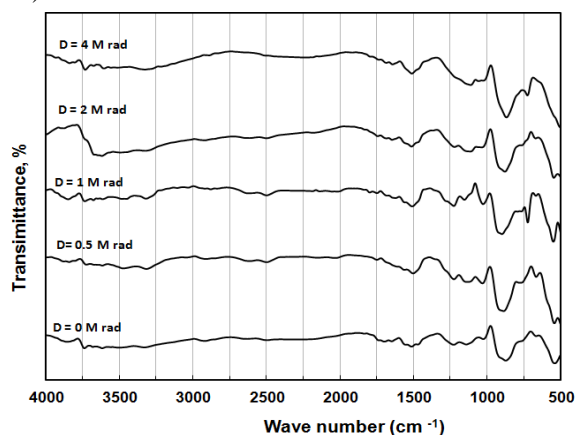
Fig. 2 FT-IR pattern for CuI-PVA/PEDOT: PSS polymer nanocomposite irradiated with different gamma doses 0, 1, 2, and 4 M rad.

Intramolecular and intermolecular hydrogen bonding are expected to occur among PVA chains due to high hydrophilic forces. An important absorption peak was verified at $n = 1142$ cm^{-1}. This band has been used as an assessment tool of poly (vinyl alcohol) structure because it is a semi-crystalline synthetic polymer able to form some domains depending on preparation parameters.

One can notice a new peak appeared by gamma irradiation at $n = 720$ cm^{-1}, which characterized by methylene (CH$_2$) Rocking [23]. This new peak is very noticeable at doses 1 and 4 M rad, while is not noticeable at doses 0.5 and 2 M rad.

Table 2 FT-IR absorption bands positions (in Cm^{-1}) and their assignments for PVA and CuI-PVA/PEDOT: PSS polymer nanocomposite irradiated with different gamma radiation doses.

Assignment	Virgin PVA	un-irradiated composite	0.5 M rad	1 M rad	2 M rad	4 M rad
CO symmetric stretching	925	973	978	979	974	972
C–O stretching	1096	1054	1077	1078	1070	1075
CH wagging	1142	1185	1189	1182	1193	--
CH2 out of plane bending	1326	1336	1389	1385	1378	1342
O–H and C–H bending	1565	1540	1544	1551	1595	1591
C=C stretching	1647	1667	--	1667	1667	1664
C=O stretching	1760			1776		1780
CH2asymmetric stretching	2933	2988	2986	2993	2986	2920
O–H stretching	3455	3398	3384	3392	3371	--

3.3 SEM Investigation

Scanning electron microscopy (SEM) investigation has been used to study the morphology of sample surface and the compatibility between various components of the polymer nanocomposites through the detection of phase separations and interfaces. However, SEM of the gamma irradiated samples with different doses between 0 and 4 M rad has been investigated, see Fig. 3. The image of TMED free CuI-PVA/PEDOT: PSS, Fig. 3.a, illustrates white particles like stones with irregular shapes dispersed in the dark field which reflects the morphology and surface roughness of such sample. As the composites were modified with ligand and subjected to gamma radiations (0 – 4 M rad) (Fig. 3 b- e), a significant variation of surface is observed. Fig. 3b, illustrates the image of un-irradiated composite sample, the morphology became more homogenous with fine structure. As the samples subjected to different doses of gamma radiation, Fig. 3 c-e, the surface morphology illustrates significant change.
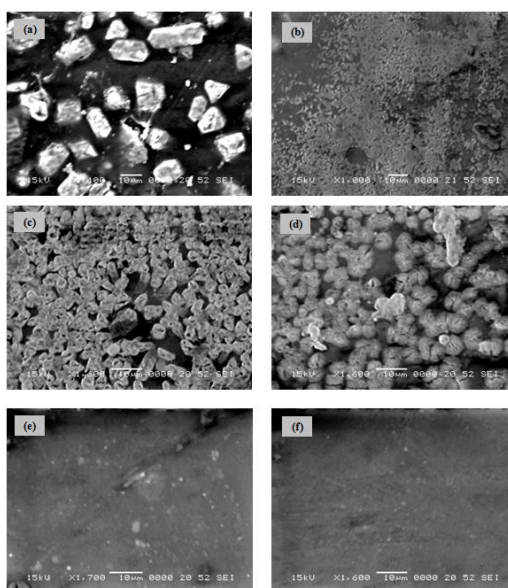
Fig. 3 SEM images for CuI-PVA/PEDOT:PSS polymer nanocomposite irradiated with different gamma doses (a) TMED free sample (b) un-irradiated sample, and gamma irradiated samples : (c) 0.5 M rad, (d) 1 M rad, (e) 2 M rad and (f) 4 M rad.

Fig. 3c illustrates clearly great roughness variation related to nano rods structure, with diameters of about 10 micron as the sample irradiated with 0.5 M rad. When the polymer composite sample subjected to higher dose, 1 M rad, a significant change of the sample surface morphology changes related to the semispherical aggregates. As the radiation dose was increased to 2 M rad a change of surface morphology to be homogenous and smooth, besides little small particles dispersed in the dark field which refer to CuI nano particles with some small holes. Further increasing of radiation dose to 4 M rad, the CuI nanoparticles dispersed on the polymer surface and became more homogenous, with some small holes which refers to the release of moisture by heating as a secondary radiation effects. In conclusion, the lower doses of gamma radiation increases surface roughness 0.5 and 1 M rad, while the medium doses results in surface smoothness. The increase of surface roughness means the increase of effective surface area which is promising for photovoltaic junction interfaces.

3.4 Thermogravimetric analysis TGA

The weight loss fraction was studied against temperature for ligand modified CuI-PVA/PEDOT: PSS polymer nanocomposite irradiated with different gamma radiation doses by using TGA at constant heating rate 10 K/min. Fig.3 illustrates the sample weight loss versus temperature for CuI-PVA/PEDOT:PSS which shows very little decrease in the mass at relatively low temperature range (less than 200 ^{o}C), this is because of dehydration.
There are two essential steps of weight loss (characterized from the second derivative of the fig. 3). The first step of weight loss is around $T_{m1} = 375$ ^{o}C, and the second one is around $T_{m2} = 490$ ^{o}C. The first step is due to water dehydration of compound water, while the second step could be attributed to hydroxyl group degradation as the onset of melting, as well as C-O decomposition associated and CO and CO_2 release.
The rate of mass loss R can be calculated according to the equation [24].

$$R = 100 \times (M_s - M_f)/M_s \ \ldots\ldots\ldots\ldots (2)$$

where, M_S and M_f are the initial and final mass at start and final temperatures of the step respectively. The different values of R at different doses of the gamma radiation are listed in Table 3. In general, one can notice that the thermal stability slightly decreased with increasing the doses of the gamma irradiation.
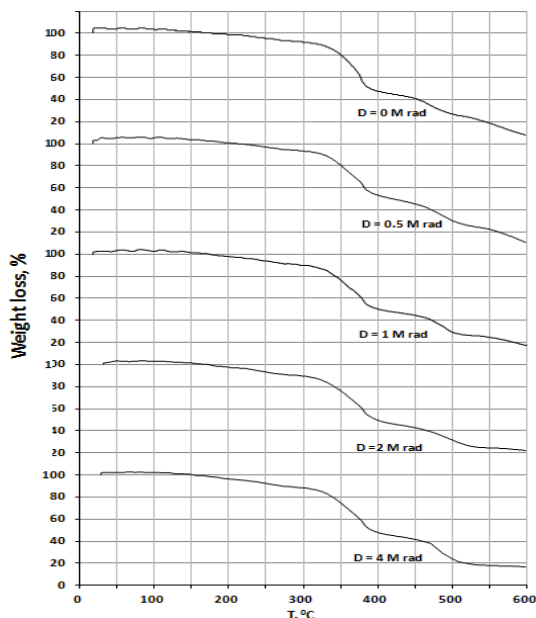
Fig. 4 Weight loss against temperature for gamma irradiated CuI-PVA/PEDOT: PSS polymer composite.

Table 3 The rate of mass loss for un-irradiated and radiated CuI-PVA/PEDOT: PSS polymer nanocomposite.

Dose / Step	Un-irradiated	0.5 M rad	1 M rad	2 M rad	4 M rad
Step 1	30.5 %	36.8 %	35.8 %	38.9 %	39.3 %
Step 2	23.4 %	30.7 %	25.6 %	25.5 %	36 %

4. AC Conductivity

The frequency dependence of ac conductivity, σ_{ac}, for irradiated of CuI-PVA/PEDOT: PSS polymer nanocomposite by 0.5 M rad at different temperatures is depicted in Fig. 5. The figure shows that ac conductivity of the polymer composite increases with frequency, which is the common characteristic of disordered materials and also increases with temperature. Both un-irradiated and irradiated samples under investigation show similar trend.
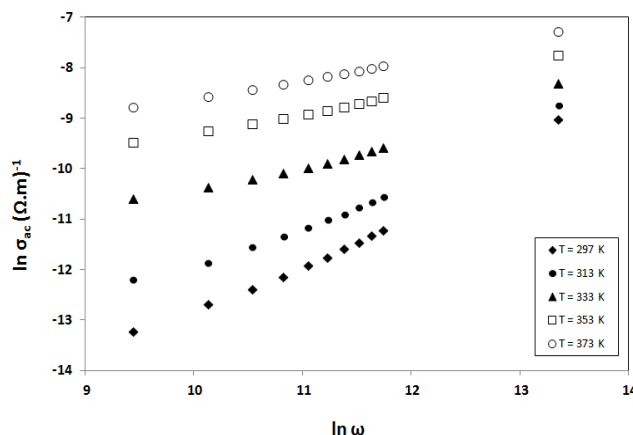
Fig. 5 The frequency dependence of ac conductivity, σ_{ac}, for irradiated CuI-PVA/PEDOT: PSS polymer nanocomposite by 0.5 M rad at different temperatures, (T= 297,313,333,353 and 373 K).

Furthermore, it is obvious that, the ac conductivity was found to increase for γ-irradiated samples in comparison to un-irradiated sample, as shown in Fig. 6. It can be observed that the value σ_{ac} for the sample irradiated by 2 M rad increases compared with the un-irradiated sample and reaches the highest ac conductivity by factor 194 % at room temperature.

Current literature on polymer exposure to gamma irradiation suggests two simultaneous mechanisms, chain scission and cross-linking [25]. The decrease in σ_{ac} (for samples irradiated by doses 1 and 4 M rad) can be attributed to an initial rate of cross-linking being greater than the rate of chain scission. The crosslinking resulted in a decrease in the mobility of the free charge carriers, which decreases the value of σ_{ac}. Also, this decrease may be attributed to the new chemical bond which formed by radiation, which confirmed by FT-IR. The increase of conductivity of irradiated CuI-PVA/PEDOT: PSS polymer nanocomposite by 2 M rad can be attributed to, free radical formation dominates and the rate of chain scission overtakes that of cross-linking, thus causing a increase in conductivity. On other hand, the increase in σ_{ac} can be attributed to the reduction of the crystalline regions in PVA and enhance the amorphous region, thereby allowing more charge carriers to participate in the conduction, as confirmed by XRD.
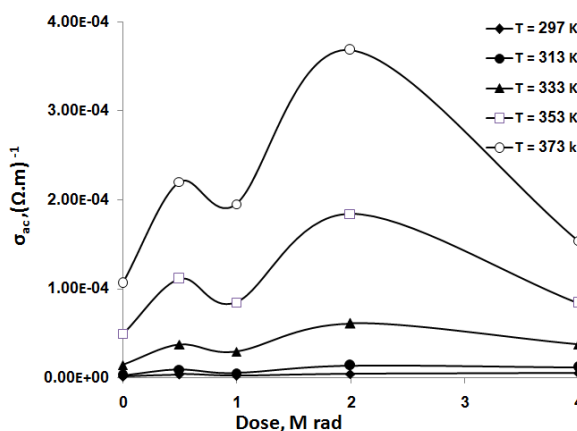
Fig. 6 The relation between σ_{ac} and γ-doses at 6 KHz for T= 297,313,333,353 and 373 K.

However, the common behavior of polymer materials is frequency dependent ac conductivity that follows a universal power law [26].

$$\sigma_{ac} = A \, \omega^S \qquad (3)$$

where, A is a frequency independent pre-exponential factor, ω is the angular frequency and s is the frequency exponent with the value in the range of $0 < s < 1$. The values of the exponent s for both un-irradiated and irradiated samples at various temperatures have been obtained using the least square fitting. The specific characteristics of the polymeric materials are depend on many factors, such that the structural properties of the polymer chains, the morphology of conduction paths of various lengths, the density of states and the mobility of electric charge carriers. The interplay between these factors leads to different values of σ_{ac} and power exponent s, which can be even larger than unity [27].
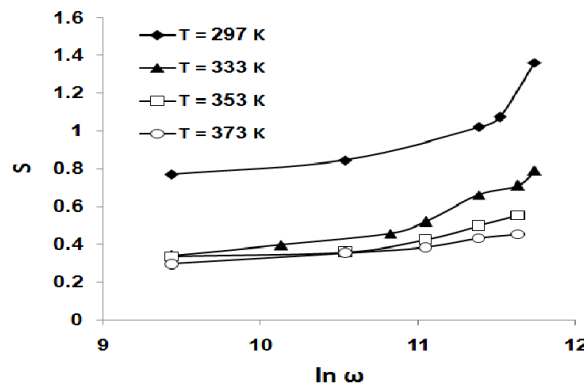
Fig. 7 The power exponent s as a function of frequency at different temperatures, (T=297,333,353 and 373K).

It can be observed in Fig. 7 that the exponent s lies in the range $0.76 < s < 1.36$ at room temperature. Also, it can be observed that the values of s decreases with temperature and increases with frequency. This shows that the correlated barrier hopping (CBH) model is the most suitable model to characterize the electrical conduction mechanism for the present polymeric system.

Fig. 8a illustrates the temperature dependence of ac conductivity for irradiated sample by 0.5 M rad at different frequencies, which can be described by the following Arrhenius equation:

$$\sigma_{ac} = \sigma_0 \, \exp (\, -E_a/kT \,) \qquad (4)$$

where, σ_0 a pre-exponential factor, E_a is the electrical activation energy, k is Boltzmann's constant and T is absolute temperature. It is seen from Fig.8a that, the ac conductivity increases with temperature for a given fixed frequency. The values of activation energy for different frequency have been calculated from the slope of the conductivity versus temperature curves.
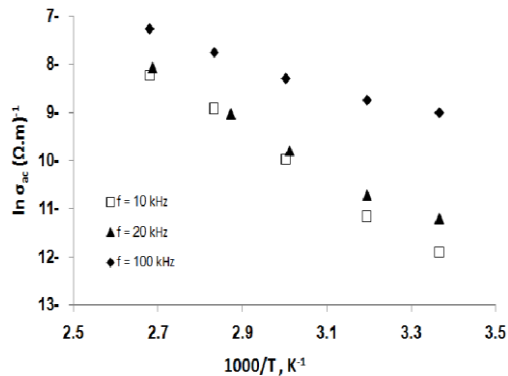
Fig. 8 (a) The temperature dependence of ac conductivity for irradiated sample by 0.5 M rad at different frequencies, 10, 20 and 100 KHz.
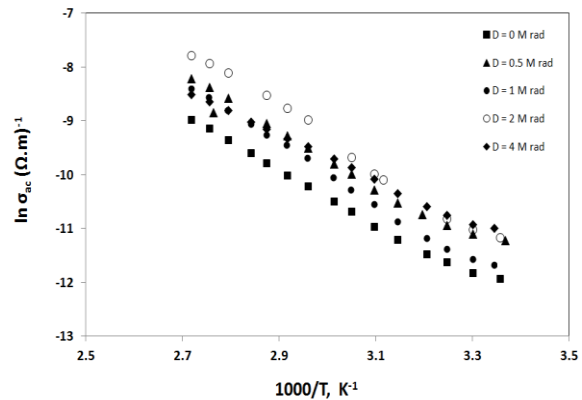
Fig. 8 (b) The variation of ac conductivity with temperature for different gamma irradiation doses at 20 KHz. different temperatures, T= 297, 313, 333 and 353 K.

The values of E_a for irradiated samples by 0.5 M rad are 0.477, 0.414 and 0.222 eV at frequencies 10, 20 and 100 K Hz respectively. The variation of conductivity with temperature can be understood in terms of hopping of charge carriers between the randomly distributed trapping centers. Moreover, its clear from the above that the activation energy E_a decreases with increasing frequency. This suggests that the applied field frequency enhances the ionic jumps between the localized states, so the activation energy decreases which increases the conductivity [28]. Fig. 8b shows the variation of conductivity with temperature for different gamma irradiation doses at 20 KHz. The calculated E_a values are listed in Table 1.

4.1 Dielectric permittivity

The real (ε') and imaginary (ε'') parts of dielectric permittivity for irradiated sample by 2 M rad as a function of frequency at different temperatures are shown in Fig. 9 and Fig. 10 respectively. The value of ε' decreases rapidly with increasing frequency. This could be attributed to the inability of the dipolar molecules in the polymer to response with increasing the rates of the applied field. The observed increase in dielectric constant towards the low frequency region is attributed to the interfacial polarization [29].
 It is also observed that dielectric permittivity (ε' and ε'') increases with temperature, which can be attributed to the increase in charge carrier density due to the increase in the dissociation of ion aggregates. On other hand, as the temperature increased the viscosity of polymeric films is decreasing and the dipoles have sufficient energy and can orient themselves easily in the direction of the applied electric field. Also, the chain segments get sufficient thermal energy to speed up its rotational motion and consequently the increase in polarization occurs [30, 31]. Both un-irradiated and irradiated samples under investigation show similar trend.
The results of ε' as a function of γ-irradiation doses at different temperatures reveal that an increase in ε' value for irradiated CuI-PVA/PEDOT: PSS polymer nanocomposite by 2 M rad, at the full range of the temperature of interest. The increase in ε' value with the irradiation dose is attributed to the formation of some defects sites in the band gaps of polymer as a result of occurrence of chain scission. Generally, these defects may indicate sign of the existence of charge carriers traps in the band gap of the polymer; it may be capturing the charge carriers. Therefore, γ-irradiation increases the ability of the polymer to store charge.
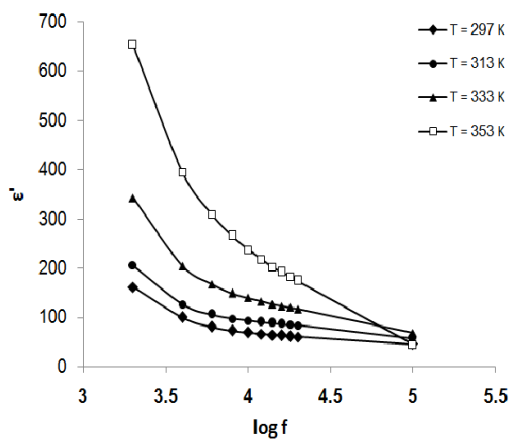
Fig. 9 The real part of dielectric permittivity (ε') for irradiated sample by 2 M rad   as a function of frequency at (a) The temperature dependence of ac conductivity for irradiated sample by 0.5 M rad at different frequencies, 10,20 and 100 KHz
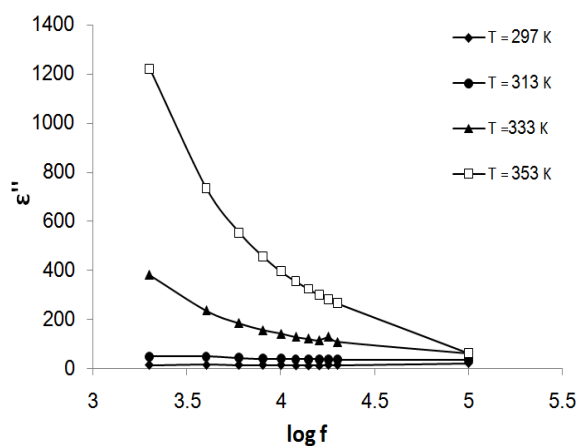
Fig. 10 Imaginary part of dielectric permittivity (ε'') for irradiated sample by 2 M rad as a function of frequency at different temperatures, T= 297,313,333 and 353K.

IV.   Conclusion

The 2 M rad γ-irradiation has significantly enhanced both the dielectric permittivity and ac conductivity of CuI-PVA/PEDOT: PSS polymer nanocomposite due to chain scissioning. FT-IR result showed a new chemical bond (CH_2 methylene Rocking) at 720 cm^{-1} for doses 1 and 4 M rad which formed by radiation, indicating the cross-linking of polymer. XRD pattern reveal a new crystalline phase (salesite) inside the polymer composites upon irradiation. The surface morphology of the irradiated films changes as compared to un-irradiated film. The ac conductivity behavior is found to obey the universal power law and interpreted in terms

of the correlated barrier hopping (CBH) model. Based on the obtained results, it can be stated that γ-Irradiation is a useful technique to control the physical properties of CuI-PVA/PEDOT: PSS polymer nanocomposite.

References

[1]   Godovsky D.Y., Adv. Polym. Sci. (2000), 153, 163–205.
[2]   El-Sayed M.A., Acc. Chem. Res. (2001) 34, 257-264.
[3]   Coakley K. M., Liu Y., Goh C., McGehee M.D., MRS Bull. (2005), 30, 37-40.
[4]   Abdelkader A., Anwar Z., J.Appl. Polym. Sci. (2006), 2, 1146-1151.
[5]   G.R.R.A. Kumara, A. Konno, G.K.R. Senadeera, P.V.V. Jayaweere, D.B.R.A. De Silva, T. Tennakone, Sol. Energy Mater. Sol. Cells 69 (2001) 195-199.
[6]   Tonooka K., Shimokawa K., Nishimura O., Thin Solid Films, (2002), 411, 129-133.
[7]   Sunetra L. Dherea, Sanjay S. Latthea, Charles Kappensteinb, Mukherjeec S.K., Venkateswara Raoa A., Appl. Surf. Sci., (2010)**,** 256, 12, 3967-3971.
[8]   Sharma G.D., Shanap T.S., Patel K.R., El-Mansy M.K., Mat. Sci.- Poland (2012), 30, 10- 16.
[9]   El-Mansy M.K., Sheha E., Patel K.R., Sharma G.D., OPTIK , **2013**, 124, 1624-1631.
[10]   Makled M.H., Sheha E., Shanap T.S., El-Mansy M.K., J. of advanced research, (2013), 4 (6), 531-538.
[11]   Y. Kima, J. Lee, H. Kang, G. Kim, N. Kim, K. Lee, Sol. Energy Mater.Sol.Cells 98(2012)39-45.
[12]   E. Sheha, Mona Nasr and M. K. El-Mansy, Phys. Scr. 88 (2013) 035701 (8pp)
[13]   N. García-Huete, et al, Radiation Physics and Chemistry 102 (2014) 108–116
[14]   Bhattacharya, A., Prog. Polym. Sci. 25, (2000), 371-401.
[15]   Luo, S., Netravali, A.N., J. Appl. Polym. Sci. 73,(1999), 1059–1067.
[16]   Chmielewski, A.G., Haji-Saeid, M., Ahmed, S., Methods Phys. Res. B 236, (2005) 44–54.
[17]   Cleland, M.R., Parks, L.A., Cheng, S., Nucl. Instr. Methods B 208, (2003), 66–73.
[18]   Zahran, A.R.R., Kandeil, A.Y., Higazy, A.A., Kassem, M.E., J. Appl. Polym Sci. 49,(1993), 1291–1297.
[19]   S. Raghu, Subramanya Kilarkaje, Ganesh Sanjeev, G.K. Nagaraja, H. Devendrappa, Radiation Physics and Chemistry 98 (2014) 124–131.
[20]   Kumar, R., Prasad, R., Vijay, Y.K., Acharya, N.K., Verma, K.C., De, Udayan, Nucl.Instrum. Methods B 212, (2003), 221–227.
[21]   R.M. Hodge, G.H. Edward, G.P. Simon, Polymer 37 (1996) 1371–1376.
[22]   Cullity, B.D, Stock, S.R, Elements of X-ray Diffraction, 3rd ed Prentice Hall, New York, (2001).
[23]   B. Stuart, Infrared Spectroscopy: Fundamentals and Applications, John Wiley,(2004).
[24]   T. Hatakeyama, F.X. Quinn, Thermal Analysis Fundamentals and Applications to Polymer Science, 2nd, John Wiley & Sons Ltd, (1999).
[25]   Woods RJ, Pikaev AK. Applied radiation chemistry: radiation processing. New York: John Wiley & Sons, Inc.; (1994).
[26]   A.K. Jonscher, Nature 267 (1977) 673.
[27]   A.N. Papathanassiou, I. Sakellis and J. Grammatikakis Appl. Phys. Lett. 91, (2007), 122911.
[28]   B. Chandar, V. Veeravazhuthi, S. Sakthivel, D. Mangalaraj, S.K.Narayandass Thin Solid Films 348 (1999) 122.
[29]   Rajendran S, Sivakumar M , Subadevi R, Mater Lett 58: (2004), 641-649.
[30]   A. Hassen, A.M. El Sayed, W.M. Morsi, S. El-Sayed, J. Appl. Phys. 112 (2012)093525.
[31]   T.A. Hanafy, J. Appl. Polym. Sci. 108 (2008) 2540–2549.